

# PROCEEDINGS OF SPIE

[SPIDigitalLibrary.org/conference-proceedings-of-spie](https://SPIDigitalLibrary.org/conference-proceedings-of-spie)

## Generation of modulation instability-induced high-repetition-rate pulse train with high-phase modulation depth

Aleksei Abramov, Igor Zolotovskii, Vladimir Kamynin, Andrei Domanov, Aleksandr Alekseev, et al.

Aleksei Abramov, Igor Zolotovskii, Vladimir Kamynin, Andrei Domanov, Aleksandr Alekseev, Dmitriy Korobko, Marina Yavtushenko, Andrei Fotiadi, "Generation of modulation instability-induced high-repetition-rate pulse train with high-phase modulation depth," Proc. SPIE 12142, Fiber Lasers and Glass Photonics: Materials through Applications III, 1214211 (25 May 2022); doi: 10.1117/12.2622312

**SPIE.**

Event: SPIE Photonics Europe, 2022, Strasbourg, France

# Generation of modulation instability-induced high-repetition-rate pulse train with high phase modulation depth

Aleksei Abramov<sup>a</sup>, Igor Zolotovskii\*<sup>a</sup>, Vladimir Kamynin<sup>b</sup>, Andrei Domanov<sup>a</sup>, Aleksandr Alekseev<sup>a</sup>, Dmitry Korobko<sup>a</sup>, Marina Yavtushenko<sup>a</sup>, Andrei Fotiadi<sup>a,c</sup>

<sup>a</sup>Ulyanovsk State University, 42 Leo Tolstoy Street, Ulyanovsk 432970, Russia; <sup>b</sup> Prokhorov General Physics Institute of the Russian Academy of Sciences, 38 Vavilov st., Moscow, 119991, Russia; <sup>c</sup>Electromagnetism and Telecommunication Department, University of Mons, Mons, B-7000, Belgium

## ABSTRACT

In this work we investigated the possibility of generating subpicosecond pulses as a result of a modulation instability of continuous wave signals with a large modulation depth. In our case a large modulation depth of a continuous wave is achieved by using a cylindrical waveguides with a running refractive index wave (RRIW). Here, the entire cascade fiber system is a cylindrical waveguides RRIW connected in series with a section of passive fiber with anomalous dispersion. To achieve high peak power values in the generated pulse train, it is necessary to add a section of active fiber with normal dispersion to the stage. It is shown that, as a result of the regime of a induce modulation instability, pulses with a peak power that are orders of magnitude higher than the power of the incoming pump wave can be formed.

**Keywords:** running refractive index wave; whispering gallery mode; frequency pulse modulation; modulation instability; high peak power generation.

## 1. INTRODUCTION

Propagation of a light pulse in a waveguide with a running refractive index wave (RRIW) is accompanied by effects that are not realized in waveguides without a RRIW [1,2]. In particular, the generation of soliton-like pulses due to modulation instability in such waveguides is studied [3,4]. In addition, the formation of azimuthal whispering gallery modes (AWGM) in such waveguides is of great interest [5,6]. It is shown that AVGM, propagating over the surface of a cylindrical silica fiber, moves along a spiral trajectory with a certain even step. Typical values of the longitudinal group velocity (along the waveguide axis) of helical waves are usually much less than the speed of light in vacuum [6]. However, it can be close to the RRIW velocity, which leads to a pronounced resonant interaction between the BVPP and the AWGM. As a result of this interaction, regular trains of optical pulses can be formed. This effect was theoretically considered in [7, 8] for waveguides with RRIW. The operation mechanism involves a proper combination of the frequency modulation and modulation instability regime (MI) that are simultaneously experienced by the input continuous wave signal as it propagates through the cylinder waveguide following the spiral trajectory. It is important to note that the MI in a considered cylindrical waveguide with RRIW differs significantly from the MI observed in standard optical fibers [9-12].

It is described by the same equation as that commonly used for describing dynamics of the Bose–Einstein condensate (BEC) [11,13] and formation of the giant pulses is similar to formation of the BEC waves reported earlier for the magnetic trap with parabolic potential near Feshbach resonance [14]. Comprehensive studies of pulse train formation have shown that the peak power of the output pulses can be orders of magnitude higher than the peak power of the input pulses.

In this paper, we explore a new approach to the application of the cylindrical waveguide structure with RRIW for the generation of optical pulse trains. In this approach, the cylindrical waveguide is just a part of the cascaded optical fiber configuration comprising also passive and active optical fiber segments. In this configuration system, the waveguide structure with RRIW is responsible mainly for the frequency modulation of the propagating AWGM light. Whereas the passive fibers with the anomalous group velocity dispersion (GVD) are mainly used as a media with MI. The segment of active fiber is employed for the power scaling of the propagating light. The proposed optical system

made it possible to generate a pulse train consisting of picosecond pulses with a kilowatt peak power from weakly modulated continuous radiation with a power of 10 mW used as an input signal.

## 2. LIGHT WAVE PROPAGATION IN THE CYLINDRICAL WAVEGUIDE WITH RRIW

At small incident angles  $\theta$ , the direction of light wave propagation is almost perpendicular to the cylinder axis (Figure 1a), both the velocity of light wave propagation and the wavevector component along the cylinder are very small, so  $V_z \ll c/n_0$  and  $\beta_z \ll \beta$ . In this case, the wave electric field could be expressed as:

$$E(z, t, r, \varphi) = A(z, t) \Phi(z, r, \varphi) \exp\left(i\omega t - i \int_0^\xi \beta d\xi\right) + c. c., \quad (1)$$

where  $A(z, t)$  is the slowly varying amplitude describing propagation of the AWGM field along the cylinder,  $\Phi(z, r, \varphi)$  is the AWGM mode profile,  $r, \varphi$  are the radial and azimuthal coordinates,  $\xi$  is the coordinate along the spiral trajectory linked with  $z$  as  $d\xi \approx Ndz = dz/\sin\theta$ ,  $N = 1/\sin\theta = V_g/V_z$  is the deceleration coefficient.

To get resonance between the AWGM and RRIW, the velocity of light wave propagation along the cylinder  $V_z$  should equal the RRIW group velocity  $V_m$ , i.e.  $V_z \approx V_m$ . In this case, the interaction between AWGM and RRIW is described as [7, 8]:

$$\frac{\partial A}{\partial \xi} - i \frac{d_2^{(1)}}{2} \frac{\partial^2 A}{\partial \tau^2} - i \frac{d_3^{(1)}}{6} \frac{\partial^3 A}{\partial \tau^3} + i R^{(1)} |A|^2 A = i \beta^{(1)} m \cos[\Omega(\tau - \delta\tau)] A - (\beta^{(1)}/Q) A, \quad (2)$$

where  $\tau = t - \int_0^\xi d\xi/V_g^{(1)}$  is the time within the running time frame,  $\beta^{(1)} = n_0^{(1)}\omega_0/c$  is the AWGM propagation constant in the waveguide with RRIW,  $V_g^{(1)} = (\partial\omega/\partial\beta^{(1)})_{\omega_0}$  is the group velocity of light propagating along the spiral trajectory with the coordinate  $\xi$ ,  $d_j^{(1)} = (\partial^j \beta^{(1)}/\partial\omega^j)_{\omega_0}$  are the second- and third-order dispersion parameters ( $j = 2, 3$ ),  $R^{(1)}$  is the Kerr nonlinear coefficient,  $Q$  is the AWGM  $Q$ -factor determining losses along  $\xi$ ,  $\delta\tau$  is the time detuning due to mismatching of the pulse group velocity and RRIW velocity, where  $\delta\tau = (\sin\theta/V_m - 1/V_g)\xi$ .

For further consideration the realistic values of the parameters used in Eq. (2) should be taken into account. Let the RRIW be an acoustic wave propagating in the silica cylinder excited externally. In this case, the RRIW phase velocity is  $V_m = 6000$  m/s and the refractive index  $n \approx 1.5$  [15]. Therefore, the resonance between AWGM with RRIW is provided with the angle of  $\theta \approx V_m n / c \approx 3 \cdot 10^{-5}$ . Specifically, the AWGMs induced in pure silica cylinder exhibit extremely high  $Q$ -factors (typically  $\sim 10^9$  [16,17]) enabling rather long optical path in the near-IR range  $\xi_0 \sim Q\lambda_0/3 \leq 300$  m. This length along the spiral trajectory corresponds to the length along the cylinder  $l \sim n_0 V_m \xi / c \sim 3 \cdot 10^{-5} \xi \leq 1$  cm.

In general, while propagating through the cylinder, the selected AWGM experiences the frequency modulation and nonlinear interaction described by the corresponding terms in Eq. (2). Since the cylindrical waveguide is used as a part of the cascaded optical fiber configuration responsible for the frequency modulation only, the nonlinear effects in the cylinder waveguide should be minimized by keeping the power level of the input optical signal as low as  $P_0 \sim 10$  mW. Besides, the cylindrical waveguide with RRIW is assumed to be of normal GVD. In this case, the light complex amplitude at the cylinder output could be expressed as

$$A(z = l, \tau) \approx A_s(\tau) \exp[i\delta(l) \cos(\Omega\tau)], \quad (3)$$

where  $A_s$  is a weakly modulated amplitude,  $\delta(l) \approx m\beta\xi \approx m\omega_0 l / V_m$  is the dimensionless parameter characterizing the

phase modulation depth. With the standard modulation depth  $m \sim 10^{-4} - 10^{-6}$ , the wave propagation constant  $\beta = 2\pi n / \lambda_0 \approx 6 \cdot 10^6 \text{ m}^{-1}$  (at  $\lambda_0 \approx 1.55 \mu\text{m}$ ) and optical path of tens of meters the phase modulation depth gets  $\delta \gg \pi / 2$ .

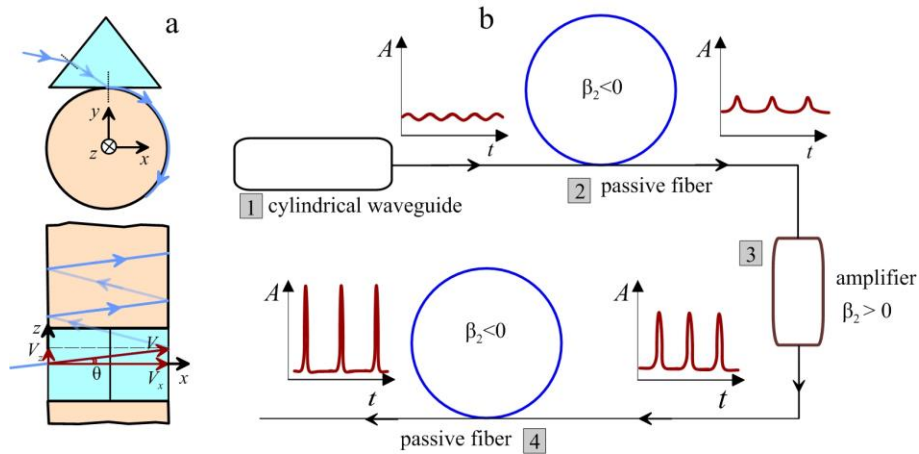


**Figure 1.** a - Geometry of optical radiation entering the cylindrical waveguide (waveguide cross section and view top of the prism). Here is  $\theta$  is the angle between the direction of radiation input into the cylindrical waveguide and cylinder cross-section.  $V$ ,  $V_z$ , and  $V_x$  are the velocity and its longitudinal and transverse components, respectively. b - Cascaded system for generation of ultrashort pulse train (1 – waveguide with RRIW, 2,4 – anomalous GVD passive fiber, 3 – active fiber with a positive GVD).

### 3. CASCADED FIBER CONFIGURATION FOR SUBPICOSECOND PULSE TRAINS GENERATION

We consider the cylindrical waveguide as a part of the cascaded optical fiber configuration comprising also passive and active optical fiber segments. In this system shown in Figure 1b, the cylindrical waveguide structure with RRIW is responsible mainly for the frequency modulation of the propagating AWGM light described by Eq. (2). The passive optical fibers with the anomalous group velocity dispersion (GVD) are used mostly as MI media for pulse shaping. The active (gain) fibers with normal dispersion are employed for peak power scaling. The spliced configuration as a whole enables the generation of high peak power pulse trains.

In general, the light propagation in the passive and active fiber segments is described by the Schrödinger equation [18-20]:

$$\frac{\partial A}{\partial z} - i \frac{d_2^{(2)}(z)}{2} \frac{\partial^2 A}{\partial \tau^2} - i \frac{d_3^{(2)}(z)}{6} \frac{\partial^3 A}{\partial \tau^3} + i R^{(2)}(z) \left( |A|^2 - \tau_R \frac{\partial |A|^2}{\partial \tau} \right) A = g(z) A, \quad (4)$$

where  $g(z)$  is the gain factor,  $\tau_R$  is the nonlinear response time characterizing the Raman self-scattering.

For standard uniform fibers, under the conditions of unsaturated optical gain in an active fiber ( $g = \text{const}$ ), negligible Raman self-scattering,  $d_3^{(2)} \rightarrow 0$  and arbitrary boundary conditions, Eq. (6) is reduced to the Gross–Pitaevskii equation:

$$\frac{\partial \bar{A}}{\partial z} - i \frac{d_{2ef}(z)}{2} \frac{\partial^2 \bar{A}}{\partial \tau^2} + i R_{ef}(z) |\bar{A}|^2 \bar{A} = -i S(z) \tau^2 \bar{A}, \quad (5)$$

where  $\bar{A}(\tau, z) \approx A(\tau, z) \exp[-i\delta \cos(\Omega\tau) - Gz]$ ,  $\tau' = f(z)\tau$ ,  $G = g - \alpha d_2^{(2)}$ ,  $S(z) = 2\alpha^2 d_2^{(2)} f^{-2}(z)$ ,  $d_g(z) = d_2^{(2)} f^2(z)$ ,  $f(z) = \exp(-2\alpha d_2^{(2)} z)$ ,  $R_f = R^{(2)} \exp(2gz)$  and  $\alpha = \delta \Omega^2 / 2$ .

In the next sections, we will explore transformation of a low power weakly modulated light propagating through four system cascades into the train of picosecond pulses with a kilowatt peak power. The numerical simulations are performed using the Split Step Fourier method [21]. Simulations of the input light transformation into the frequency modulated low amplitude pulses in the cylindrical waveguide (cascade 1) are based on Eq.(1). The processes of MI and optical amplification in the fiber cascades 2-4 are simulated basing on Eq.(4). It is worth noting that the simplified Eq.(5) is also used for an advanced determination of the fiber point, where the peak pulse amplitude gets its maximum. This point depends on the phase modulation depth  $\delta(l) \approx m\beta\xi \approx m\omega_0 l / V_m$  and is determined as the point  $z_{comp}$  of Eq.(5) singularity [8]:

$$z_{comp} \approx \left| \frac{2}{\delta(l)\Omega^2 d_2^{(2)}} \right| \approx \left| \frac{2V_m}{mn_0^{(1)}\omega_0\Omega^2 l d_2^{(2)}} \right|. \quad (6)$$

The first element of the considered cascaded configuration is a cylindrical waveguide with RRIW. It is used to convert the input CW light into a train of phase modulated pulses possessing negligible intensity amplitude. Introduced at a small angle into the waveguide, the input light covers the optical path  $\xi$  along a spiral trajectory acquiring a deep frequency modulation characterized by a dimensionless parameter  $\delta \gg \pi / 2$ .

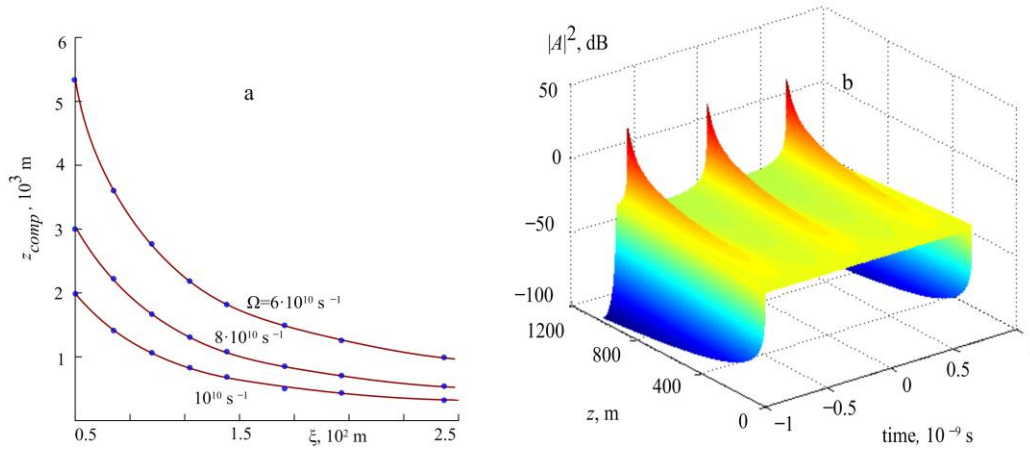


Figure 2. a - Critical length of the anomalous GVD fiber as a function of the optical path  $\xi$  in the cylindrical waveguide with RRIW at different modulation frequencies  $\Omega$ . b - Time profile of the optical signal propagating in the passive optical fiber (cascade 2).

Then the light pulses formed in cascade 1 propagate through the fiber possessing anomalous GVD. At this stage, the light pulses transform into a train of amplitude pulses with the repetition rate  $\Omega$ . If the fiber is long enough the formed pulse train becomes well pronounced with a distinctive separation into individual subpicosecond pulses. The fiber length corresponding to this case is estimated from (6) and depends on the fiber GVD, modulation frequency, and frequency modulation depth. The numerical simulation results shown in Fig.2a are in good agreement with the simplified Eq.(6).

We consider a narrow-band quasi-continuous weakly modulated signal introduced into cascade 1 that is expressed as [7,8,21]:

$$A(z^{(1)} = 0, \tau) \approx \sqrt{P_0} [1 + \Delta \cos(\Theta\tau)], \quad (7)$$

where  $\Delta = 10^{-4}$  is the input signal modulation depth,  $\Theta = 10^{12} \text{ s}^{-1}$  is the input signal modulation frequency. The cylindrical waveguide dispersion parameters used for calculations are  $d_2 = 10^{-26} \text{ s}^2/\text{m}$ ,  $d_3 = 10^{-41} \text{ s}^3/\text{m}$ ,  $m\beta = -10 \text{ m}^{-1}$ ,

$\xi = 300$  m,  $\Omega = 4 \cdot 10^9$  s<sup>-1</sup>, the length of light propagation in the cylinder waveguide is  $l \approx 1$  cm, and the input optical signal power is  $P = 0.1$  W. The final frequency modulation depth is  $\delta \approx -3 \cdot 10^3$ . We assume the AWGM  $Q$ -factor in the cylinder waveguide to be  $\sim 10^9$ . The passive fiber dispersion parameters are:  $d_2 = -10^{-26}$  s<sup>2</sup>/m;  $d_3 = 10^{-40}$  s<sup>3</sup>/m. In all cascade elements the Kerr nonlinearity and nonlinear response time are assumed to be  $R^{(2)} = 3 \cdot 10^{-3}$  W<sup>-1</sup>m<sup>-1</sup> and  $\tau_R = 3 \cdot 10^{-15}$  s respectively. In this case, an ultrashort pulse train is generated at the length of 800 m as shown in Fig. 2b.

One can see that the peak power increases sharply at the final fiber length during the short time interval. At the cascade 2 output, the peak power is more than two orders of magnitude higher than the power of input signal introduced into the system. We have found that under the used conditions the input signal modulation depth (in the range of  $10^{-6} - 10^{-1}$ ) does not affect the dynamics of ultrashort pulse formation. In order to generate a train of pulses with higher peak power, an active fiber (amplifier) and a section of passive fiber are added into the system as the third and fourth fiber cascades as shown in Figure 2. While propagating in the pumped active fiber the formed pulses experience amplification and the pulse peak power increases adiabatically. In the last system cascade, the amplified pulses are finally compressed. Using this technique, the pulse train peak power could be drastically increased without deformation of the pulse shape. The parameters used for numerical simulations are the same for the active (cascade 3) and passive (cascades 2, 4) fibers, except for the normal GVD  $d_2 = 10^{-26}$  s<sup>2</sup>/m [22] used for the active fiber.

Let us consider the pulse train generation in the cascaded configuration with different passive fiber lengths (cascade 2): 50 (a), 500 (b), 1000 m (c, d) and the active fiber (cascade 3) length of 10 meters (Figure 3). One should note that initial formation of pulses from the frequency modulated light occurs at relatively short fiber lengths  $< 10$  m. Evolution of the pulse shape in the considered cascade is shown in Figure 3 (left). The corresponding pulse shapes at the input of cascade 2 and system output are presented in Figure 3 (right). The gain bandwidth is  $\Delta\omega_i = 10^{12}$  s<sup>-1</sup> for (a-c) and  $\Delta\omega_i = 4 \cdot 10^{13}$  s<sup>-1</sup> (d). Dashed lines are the peak power of generated pulses.

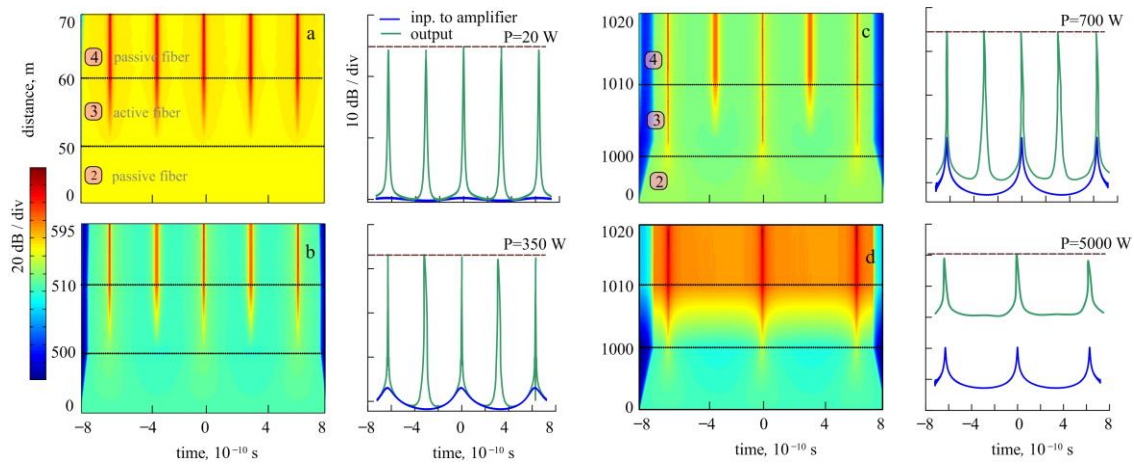


Figure.3. Evolution of time envelope profile in the fiber cascade (2-4) with different passive fiber lengths (cascade 2): 50 (a), 500 (b), 1000 m (c, d) and amplifier length of 10 meters. Time profiles of pulse trains in semi-logarithmic scale at the amplifier input (blue curves) and output (green curves). Gain bandwidth is  $\Delta\omega_i = 10^{12}$  s<sup>-1</sup> (a-c) and  $\Delta\omega_i = 4 \cdot 10^{13}$  s<sup>-1</sup> (d) at  $g = 0.3$  m<sup>-1</sup>.

## 4. CONCLUSION

In this study, we have demonstrated generation of the subpicosecond pulses in the cascaded fiber configuration comprising (as cascade 1) the cylindrical waveguide with RRIW responsible for initial formation of the CW light with a deep frequency modulation  $\delta \gg \pi/2$ . It is shown that the pulses with the peak power by orders of magnitude higher than the input power can be generated through the modulation instability directly from the input CW light. Similar generation of subpicosecond pulse trains with the comparable peak power level is also achievable with a low-amplitude noise signal introduced into the cylindrical waveguide. However, in this case a proper combination of the fiber system parameters such as the passive fiber length, gain bandwidth, and gain factor should be provided.

In fact, the proposed mechanism is similar to mode-locking taking place outside the source demonstrated earlier as the Fourier synthesis obtained with the self-swiping fiber lasers [23]. Specifically, the generated FM light is resistive to nonlinear perturbations and could be amplified up to high peak powers following the singular solution of Eq.(7). The reported pulse train generators are attractive for material processing laser systems, lidars, compact charged-particle accelerators, and laser isotope separation systems. In this context, the cascaded configurations comprising the cylindrical waveguide with RRIW and active graded-index large mode area ( $1000 \mu\text{m}^2$ ) fibers [24,25] are of particular interest. The train of pulses with a GHz repetition rate and peak power much higher than 1 kW could be delivered with such fibers. It is worth noting that the use of a standard pair of diffraction gratings (as cascade 4) is preferable to an anomalous dispersion fiber in this case. Importantly, the pulses considered in this work possess some similarity with the rogue waves (also known as freak waves). Such kind of phenomenon is of fundamental importance [26,27] and in the future could be also implemented with microcavities [6,28], ring lasers [21,30] or running wave modulators [29]. The considered generators of high repetition rate pulses could be promising for radio photonics technologies [31].

## REFERENCES

- [1] Sychugov, V.A. , Torchigin, V.P. , and Tsvetkov, M. Yu. "Whispering-gallery waves in optical fibres," *Quantum Electron.* 8, 738–742 (2002).
- [2] Abramov, A. S., Kadochkin, A. S., Sannikov, D. G., Zolotovskii, I. O., Yavtushenko, M. S., Moiseev, S. G., Svetukhin, V. V., and A. A. Fotiadi. "Cylindrical silicon near-IR optical amplifier driven by direct current," *J. Opt. Soc. Am. B.* 37, 2314-2318 (2020).
- [3] Zolotovskii, I. O. , Korobko, D. A. , Lapin, V. A. , and Sementsov, D. I. "Modulation instability of pulsed radiation in an optical waveguide in the presence of the traveling refractive index wave," *Opt. and Spectroscopy* 121, 277 (2016).
- [4] Gumenyuk, R., Okhotnikova, E. O., Filippov, V., Korobko, D. A., Zolotovskii, I. O. and Guina, M., "Fiber lasers of Prof. Okhotnikov: review of the main achievements and breakthrough technologies," *IEEE Journal of Selected Topics in Quantum Electronics* 24, 1-14 (2017).
- [5] McCall, S.L. , Levi, A.F.J. , Slusher, R.E., Pearnton, S.J., and Logan, R.A. "Whispering gallery mode microdisk laser," *Appl. Phys. Lett.* 60, 289-291 (1992).
- [6] Vahala, K.J. "Optical microcavities," *Nature.* 24, 839-846 (2003).
- [7] Zolotovskii, I.O., Korobko, D.A., Lapin, V.A., Mironov, P.P., Sementsov, D.I., Yavtushenko, M.S., and Fotiadi, A.A. "Generation of ultrashort laser pulses through a resonant interaction of quasi-continuous wave packet with running refractive index wave," *J. Opt. Soc. Am. B.* 36, 2877-2883 (2019).
- [8] Zolotovskii, I.O., Korobko, D.A., Lapin, V.A., Mironov, P.P. , Sementsov, D.I., Fotiadi, A.A., and Yavtushenko, M.S. "Generation of subpicosecond pulses due to the development of modulation instability of whispering-gallery-mode wave packets in an optical waveguide with a travelling refractive-index wave," *Quantum. Electron.* 48, 818–822 (2018).
- [9] Chernikov, S.V., and Mamyshev, P.V. "Femtosecond soliton propagation in fibers with slowly decreasing dispersion," *J. Opt. Soc. Am. B* 8, 1633 (1991).
- [10] Zolotovskii, I.O., Lapin, V.A., Sementsov, D.I., Fotiadi, A.A., and Popov, S.V. "Generation of high frequency trains of chirped soliton-like pulses in inhomogeneous and cascaded active fiber configurations," *Opt. Commun.* 426, 333–340 (2018).
- [11] Kivshar, Yu.S., and Agrawal, G.P. [Optical Solitons: From Fibers to Photonic Crystals], Academic Press: New York, USA, 125 (2003).
- [12] Zolotovskii, I. O., Korobko, D. A. and Lapin, V. A., "Modulation instability and short-pulse generation in media with relaxing Kerr nonlinearity and high self-steepening," *Quantum Electronics* 44, 42(2014).
- [13] Dalfovo, F., Giorgini, S., Pitaevskii, L.P., and Stringari, S. "Theory of Bose-Einstein condensation in trapped gases," *Rev. Mod. Phys.* 71, 463 (1999).
- [14] Inouye, S., Andrews, M.R., Stenger, J. et al. "Observation of Feshbach resonances in a Bose-Einstein condensate," *Nature* 392, 151 (1998).
- [15] Goutzoulis, A.P. and Pape, D.R. [Design and fabrication of acousto-optic devices], Marcel Dekker: New York, USA, 68 (1994).
- [16] Savchenkov, A., Strekalov, D., Ilchenko, V, Maleki, L., Grudinin, I., and Matsko A. "Ultra high Q crystalline microcavities," *Opt. Commun.*, 265, 33-38 (2006).
- [17] Sumetsky, M. "Nanophotonics of optical fibers," *Nanophotonics.* 2, 393 (2013).

- [18] Liu, X., Närhi, M., Korobko, D. and Gumenyuk, R., "Amplifier similariton fiber laser with a hybrid-mode-locking technique," *Optics Express* 29, 34977-34985 (2021).
- [19] Korobko, D.A., Fotiadi, A.A., Zolotovskii, I.O., "Mode-locking evolution in ring fiber lasers with tunable repetition rate," *Optics Express* 25, 21180-21190 (2017).
- [20] Ribenek, V. A., Stoliarov, D. A., Korobko, D. A. and Fotiadi, A. A., "Pulse repetition rate tuning of a harmonically mode-locked ring fiber laser using resonant optical injection," *Optics Letters* 46, 5687-5690 (2021).
- [21] Agrawal, G.P. [Nonlinear fiber optics], 4th ed.; Springer: New York, USA, 530 (2007).
- [22] Panyaev, I. S., Stoliarov, D. A., Sysoliatin, A. A., Zolotovskii, I. O. and Korobko, D. A., "High-frequency pulse train generation in dispersion-decreasing fibre: using experimental data for the metrology of longitudinally nonuniform fibre," *Quantum Electronics* 51, 427 (2021).
- [23] Lobach, I.A., Drobyshev, R.V., Fotiadi, A.A., Podivilov, E.V., Kablukov, S.I., and Babin, S.A. "Open-cavity fiber laser with distributed feedback based on externally or self-induced dynamic gratings," *Opt. Lett.* 42, 4207–4210. (2017).
- [24] Renninger, W.H., and Wise, F.W. "Optical solitons in graded-index multimode fibers," *Nat. Commun.* 4, 1719 (2013).
- [25] Krupa, K., Tonello, A., Shalaby, B. M., et al. "Spatial beam self-cleaning in multimode fibres," *Nat. Photonics*, 237 11, (2017).
- [26] Solli, D.R., Ropers, C., Koonath, P., and Jalali, B. "Optical rogue waves," *Nature* 450, 1054 (2007).
- [27] Moses, J., Malomed, B.A., and Wise, F.W. "Self-steepening of ultrashort optical pulses without self-phase modulation," *Phys. Rev. A* 76, 021802 (2007).
- [28] Korobko, D. A., Zolotovskii, I. O., Svetukhin, V. V., Zhukov, A. V., Fomin, A. N., Borisova, C. V. and Fotiadi, A. A., "Detuning effects in Brillouin ring microresonator laser," *Optics Express* 28, 4962-4972 (2020).
- [29] Kawanishi, T., Sakamoto, T., and Izutsu, M. "High-speed control of lightwave amplitude, phase, and frequency by use of electrooptic effect," *IEEE J. of Select. Top. Quantum Electron.* 13, 79-91 (2007).
- [30] Ribenek, V. A., Stoliarov, D. A., Korobko, D. A. and Fotiadi, A. A., "Mitigation of the supermode noise in a harmonically mode-locked ring fiber laser using optical injection," *Optics Letters* 46, 5747-5750 (2021).
- [31] Lim, C., Nirmalathas, A., Bakaul, M., Gamage, P., Lee, K.L., Yang, D., Novak, D., and Waterhouse, R. "Fiber-wireless networks and subsystem technologies," *J. Lightwave Technol.*, 8, 390–405 (2010).